PCCP

Columnar phases and field induced biaxiality of a Gay–Berne discotic liquid crystal

Roberto Berardi, Silvia Orlandi and Claudio Zannoni

Dipartimento di Chimica Fisica ed Inorganica, Università, Viale Risorgimento 4, 40136 Bologna, Italy

Received 28th February 2000, Accepted 25th April 2000
Published on the Web 19th June 2000

We have studied a system of discotic particles with a central transverse dipole using Monte Carlo (MC) computer simulations at constant pressure. We have investigated several temperatures corresponding to nematic and columnar liquid crystal phases and determined the molecular and dipolar organizations. Low temperature columnar phases are characterized by local biaxial ordering of dipoles, even if the system is on the whole uniaxial. However, simulations in the presence of a transverse field for different field and dipole strengths show that the system has a large susceptibility and easily becomes biaxial, making it potentially interesting for switching applications. An explicit formulation for the susceptibility in terms of biaxial invariants is derived.

1 Introduction

Thermotropic discotic mesogens are now available with a variety of chemical structures.[1–8] They all share the capability of self organizing when cooling from their isotropic phase and of forming columnar aggregates. These aggregates may consist of only a few molecules with the phase formed missing long range positional order, corresponding to an ordering of a nematic type. However, and perhaps more interestingly, columnar phases with long range stacks of mesogenic molecules can also be obtained, typically at lower temperatures. The columns themselves can have a regular arrangement, *e.g.* rectangular or hexagonal, in the plane perpendicular to the column. These structures are particularly interesting since the molecules forming the columns are on one hand extremely ordered (typical order parameters $\langle P_2 \rangle \approx 0.8$–$0.9$), but at the same time they can rotate around the column axis without disrupting the stacking. Thus, even allowing for the possibility of some chain entanglement in mesogens where the core is surrounded by long tails, the motion around the axis might be sufficiently easy to allow for some useful switching by the action of a field transversal to the column axis and coupling *e.g.* to a dipole in the molecular plane.

Computer simulations of mesogen models provide an attractive way of investigating this possibility. In particular a system of Gay–Berne (GB)[9] discs or rather oblate ellipsoids has been shown to produce a rectangular columnar phase[10–12] or a hexagonal phase[13] according to the parametrization[14] adopted.

The effect of an axial point dipole has been investigated by us previously,[13] while a diffuse axial dipole ring has been studied by Patey *et al.*[15] and cut-spheres with axial dipole by Weis *et al.*[16] However, no simulations on discotic particles with a transverse dipole are available, to the best of our knowledge.

Here we investigate a system of Gay–Berne disc-like particles with an added transverse dipole without and with an external field. In particular we examine first the phases obtained by performing constant volume (MC-NVT) and constant pressure (MC-NPT) Monte Carlo simulations[17] on a system of $N = 1000$ particles. We then select a state point where the system is columnar and we investigate the susceptibility of a larger system of $N = 8000$ particles as well as the biaxial order induced by applying a transversal external field.

2 The model and its simulation

We consider a system of uniaxial oblate ellipsoidal particles with axes σ_e and σ_s, with $\sigma_e < \sigma_s$ and with an embedded transversal electric point dipole placed in the centre.[13] The pair potential is the sum of a Gay–Berne (GB)[9–14] and a dipole–dipole term: $U_{ij}^* \equiv U_{ij}/\varepsilon_s = U_{ij}^{GB*} + U_{ij}^{d*}$. The Gay–Berne term has a repulsive and attractive contribution with a 12–6 inverse distance dependence form

$$U_{ij}^{GB*} = 4\varepsilon(\hat{z}_i, \hat{z}_j, \hat{r})\left[\left\{\frac{\sigma_e}{r - \sigma(\hat{z}_i, \hat{z}_j, \hat{r}) + \sigma_e}\right\}^{12} - \left\{\frac{\sigma_e}{r - \sigma(\hat{z}_i, \hat{z}_j, \hat{r}) + \sigma_e}\right\}^{6}\right], \quad (1)$$

with the circumflex indicating a unit vector and $\hat{z}_i$, $\hat{z}_j$ defining the orientation of the principal axis of particles i and j taken along their symmetry axis, while $\boldsymbol{r} = \boldsymbol{r}_j - \boldsymbol{r}_i \equiv r\hat{\boldsymbol{r}}$ is the intermolecular vector of length r. The rather complicated anisotropic contact distance $\sigma(\hat{z}_i, \hat{z}_j, \hat{r})$ and interaction energy $\varepsilon(\hat{z}_i, \hat{z}_j, \hat{r})$ are defined as in ref. 9. We employ the same parametrization used in ref. 13 related to that used by Emerson *et al.* in ref. 10 and based on the dimensions of a triphenylene core, namely: shape anisotropy $\sigma_e/\sigma_s = 0.345$, interaction anisotropy $\varepsilon_e/\varepsilon_s = 5$, but using instead energy parameters $\mu = 1$ and $\nu = 3$ as in refs. 13 and 14. σ_s and ε_s are used as molecular units of length and energy. The cutoff radius adopted is $r_c = 1.4\sigma_s$. We have shown elsewhere that this discotic GB system, both without dipole[18] and with an axial dipole,[13] gives a discotic nematic and hexagonal columnar phase. The dipolar energy term is given by

$$U_{ij}^{d*} = \frac{\mu_i^* \mu_j^*}{r^3}\left[\hat{x}_i \cdot \hat{x}_j - 3(\hat{x}_i \cdot \hat{r})(\hat{x}_j \cdot \hat{r})\right], \quad (2)$$

where we consider transverse dipole moments $\boldsymbol{\mu}_i^* \equiv \mu^* \hat{x}_i$, $\boldsymbol{\mu}_j^* \equiv \mu^* \hat{x}_j$ (the dimensionless $\mu^* \equiv (\mu^2/\varepsilon_s\sigma_s^3)^{1/2}$). Here we have

used reduced dipole moments $\mu^* = 0.8$ and $\mu^* = 0.4$ which, when considering for instance a molecular diameter of $\sigma_s = 9.27$ Å, and an energy term $\varepsilon_s = 0.49 \times 10^{-14}$ erg, correspond to about 1.6 D and 0.8 D.†

We have first performed extensive preliminary canonical ensemble (constant number of molecules N, volume V and temperature T)[17] Monte Carlo simulations of a system of $N = 1000$ interacting particles enclosed in a cubic box with periodic boundary conditions at a reduced density $\rho^* \equiv N\sigma_s^3/V = 2.5$. We have studied the system at a series of temperatures $T^* \equiv k_B T/\varepsilon_s$ (where k_B is the Boltzmann constant) finding isotropic, nematic and columnar phases with different degrees of alignment (see Table 1 and Fig. 1).

The MC runs were started from well equilibrated configurations of the dipole-less system.[11,13] The starting orientation of the dipole in the molecular plane was chosen at random to ensure a non-ferroelectric initial phase ($\langle P_1 \rangle = 0$). Each sample was then equilibrated from a minimum of 200 kcycles to a maximum of 300 kcycles, where a cycle corresponds to N attempted moves. The production runs were usually 200 kcycles long. In order to speed up the equilibration process we have allowed the dipoles to flip 180° around the disc $\hat{z}_i$ axis. In practice flip moves are attempted with probability 0.2.

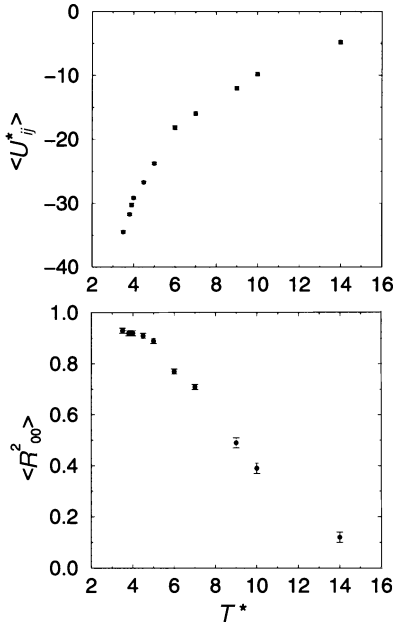

Fig. 1 Average total energy per particle $\langle U_{ij}^* \rangle = \langle U_{ij}^{GB*} \rangle + \langle U_{ij}^{d*} \rangle$ (top), and orientational order parameter $\langle R_{00}^2 \rangle \equiv \langle P_2 \rangle$ (bottom) for MC-NVT simulations at $\rho^* = 2.5$ of a system of $N = 1000$ GB discs with transverse dipole $\mu^* = 0.8$ as a function of temperature T^*.

Table 1 Results from MC-NVT simulation at density $\rho^* = 2.5$ of a system of $N = 1000$ GB discotic molecules with transversal dipole $\boldsymbol{\mu}_i \| \hat{\boldsymbol{x}}_i$ with module $\mu^* = 0.8$. We report average total energy per particle $\langle U_{ij}^* \rangle = \langle U_{ij}^{GB*} \rangle + \langle U_{ij}^{d*} \rangle$, orientational order parameter $\langle R_{00}^2 \rangle \equiv \langle P_2 \rangle$ and dielectric constant $\bar{\varepsilon}$ at temperatures T^* corresponding to isotropic (I), nematic (N) and columnar (Col_h) phases as indicated. Additional biaxial order parameters $\langle R_{02}^2 \rangle$, $\langle R_{20}^2 \rangle$ and $\langle R_{22}^2 \rangle$ are zero, within the simulation error bars, at all temperatures studied

T^*	Phase	$\langle U_{ij}^* \rangle$	$\langle R_{00}^2 \rangle$	$\bar{\varepsilon}$
3.5	Col_h	-35.3 ± 0.2	0.93 ± 0.01	1.2 ± 0.1
3.8	Col_h	-32.3 ± 0.2	0.92 ± 0.01	1.6 ± 0.1
3.9	Col_h	-30.0 ± 0.3	0.92 ± 0.01	1.6 ± 0.1
4.0	Col_h	-29.4 ± 0.2	0.92 ± 0.01	1.5 ± 0.1
4.5	Col_h	-26.9 ± 0.2	0.91 ± 0.01	1.7 ± 0.1
5.0	Col_h	-25.0 ± 0.2	0.89 ± 0.01	1.8 ± 0.1
6.0	N	-18.2 ± 0.3	0.77 ± 0.01	1.5 ± 0.2
7.0	N	-15.9 ± 0.3	0.71 ± 0.01	2.0 ± 0.2
9.0	N	-11.8 ± 0.3	0.49 ± 0.02	1.8 ± 0.2
10.0	N	-9.4 ± 0.3	0.39 ± 0.02	1.8 ± 0.2
14.0	I	-4.8 ± 0.3	0.12 ± 0.02	1.8 ± 0.2

† 1 D $\approx 3.335\,64 \times 10^{-30}$ C m.

The long range dipolar potential contributions were evaluated using the Ewald summation technique with tin foil boundary conditions[19] employing the same parameters we have used in refs. 13 and 20.

We have found, as in previous studies,[10] that at sufficiently low temperatures, *e.g.* here $T^* = 3.5$, the system develops holes. This indicates a difficulty of the system to equilibrate under the constraint of a fixed box size and shape. Constant pressure (MC-NPT)[17] simulations were thus run in the columnar phase at dimensionless pressure $P^* = P\sigma_s^3/\varepsilon_s = 5$ and selected temperature $T^* = 2.0$, 2.5, 3.0, 3.5 allowing for box shape changes, successfully eliminating residual holes. In this case the dipolar energy is computed with the reaction field technique.[21–24] The dielectric constant of the surrounding medium was $\varepsilon_{rf} = 1.5$ and the cutoff distance $r_{rf} = 3\sigma_s$. This technique is in principle less reliable than Ewald summation but considerably faster. In all cases results from reaction field runs were fully consistent with the Ewald ones, in agreement with the findings of other authors and ourselves for large mesogenic dipolar systems.[22–24]

Additional NPT simulations for larger samples of $N = 8000$ particles were run on a Cray T3E using up to 128 processors and on a IBM SP2 in order to further check the results. We implemented a replicated data structure, where each of the processors calculates the energy contribution of a subset of particles.

3 Results and discussion

Starting from highest temperature studied, the first observation is that the system is isotropic. Although this is quite predictable, checking that the system is isotropic is important to make sure that no *a priori* bias exists, towards some form of organized structure. As the temperature is reduced, orientational order develops and molecules organize in a nematic and then by further lowering T^* in a columnar hexagonal phase. Representative configurations are shown in Fig. 2.

In Table 1 we report the most important thermodynamic observables for the temperatures studied. The local director frame with axes $\hat{\boldsymbol{X}}$, $\hat{\boldsymbol{Y}}$ and $\hat{\boldsymbol{Z}} \equiv \hat{\boldsymbol{n}}$ and the orientational order parameter $\langle P_2 \rangle \equiv \langle R_{00}^2 \rangle$, were calculated as described in ref. 25. Our mesogenic particles with GB and dipolar interactions along two perpendicular (*i.e.* $\hat{\boldsymbol{x}}$ and $\hat{\boldsymbol{z}}$) axes have biaxial symmetry. Thus, we have also calculated biaxial order parameters, in particular the average biaxially symmetrized Wigner rotation matrices $\langle R_{mn}^L \rangle$,[25,26] where

$$R_{mn}^L \equiv \tfrac{1}{4}(D_{m,n}^{L*} + D_{m,n}^{L*} + D_{m,-n}^{L*} + D_{-m,-n}^{L*}). \quad (3)$$

The biaxial order parameter $\langle R_{22}^2 \rangle$, and the additional ones $\langle R_{02}^2 \rangle$ and $\langle R_{20}^2 \rangle$ were zero, within our error level, at all temperatures studied for the system in the absence of an external field. The dielectric constant $\bar{\varepsilon}$ (ref. 19) shows that the system is not ferroelectric.

We now describe the structures adopted by the sample at the different temperatures and in particular those corresponding to the snapshots in Fig. 2.

We examine first the distribution of particle centres as a function of the molecular separation r, as given by the radial correlation function $g_0(r) = 1/(4\pi r^2 \rho)\langle \delta(r - r_{ij}) \rangle_{ij}$ and its anisotropies. The $g_0(r)$ for the low temperature columnar phase ($T^* = 3.5$), shown in Fig. 3, presents several well defined

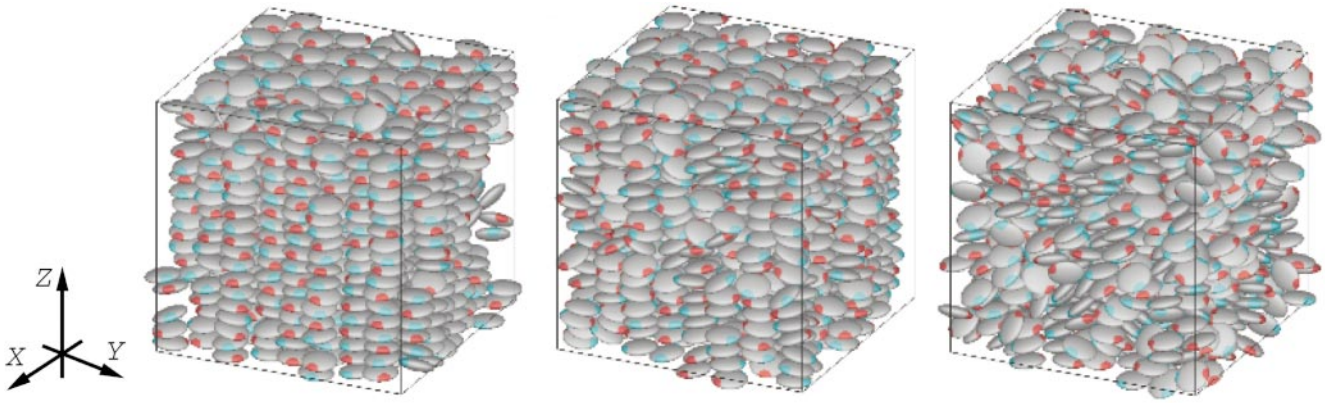

Fig. 2 Snapshots of MC-NVT configurations (side view) for systems of $N = 1000$ GB discs with transverse dipole $\mu^* = 0.8$ at density $\rho^* = 2.5$ and temperatures $T^* = 3.5$ (columnar, left), 4.5 (columnar, middle), and 7.0 (nematic, right). The red and cyan "patches" label the head and tail of the molecular dipoles. The column axis defines the $\hat{\boldsymbol{Z}}$ direction.

peaks related to the molecular organization of this mesophase. The first two maxima correspond to the first two neighbouring pairs within the same column (face-to-face). The next hump is given by the superposition of two maxima due to adjacent pairs of molecules belonging to different columns (side-by-side) and their position ($r/\sigma_s \approx 0.9$ and $r/\sigma_s \approx 1.1$) is typical of a hexagonal arrangement of interdigitated columns, also found in the axial polar[13] and apolar discotic systems. Notice, however, that at higher distances r the position of the peaks corresponds to molecules belonging either to the same or to different columns and a simple assignment is difficult and can be misleading. The hexagonal ordering is clearly shown in the snap-shots of our MC samples taken along the director $\hat{\boldsymbol{Z}}$ (shown later in Fig. 8). Less structured features are found in $g_0(r)$ for the $T^* = 4.5$ sample, the two intra-column peaks are less sharply defined and the fingerprint of the hexagonal ordering is not visible. At this temperature the columns are still arranged in a hexagonal fashion but without interdigitation. At $T^* = 7.0$ the system forms a nematic phase and the radial correlation function for the nematic phase shows no positional ordering: side-by-side configurations are approximately as frequent as face-to-face.

Further details on phase structure can be obtained by studying the second rank anisotropy $g_2{}^+(r) = \langle \delta(r - r_{ij}) P_2(\cos \beta_{ij}) \rangle_{ij}$ where β_{ij} is the angle between the intermolecular vector and the phase director $\hat{\boldsymbol{Z}}$[14,27] (Fig. 4). At the temperatures corresponding to the columnar phases the anisotropy exhibits a rich structure even for high molecular separations. For these temperatures ($T^* = 3.5$, 4.5) the columns are well defined and they extend across the whole MC sample. A closer look at the curves shows two positive maxima for the intra-column neighbouring pairs (intermolecular vector parallel to the director) and a third negative peak corresponding to side-by-side molecules belonging to adjacent columns (intermolecular vector perpendicular to the director). In the nematic ($T^* = 7.0$) phase the face-to-face clustering of particles is practically negligible except for first neighbours.

Molecular orientational correlations, particularly those reflecting dipolar, and local biaxial ordering can be studied considering a suitable set of Stone invariants[28,29] averaged

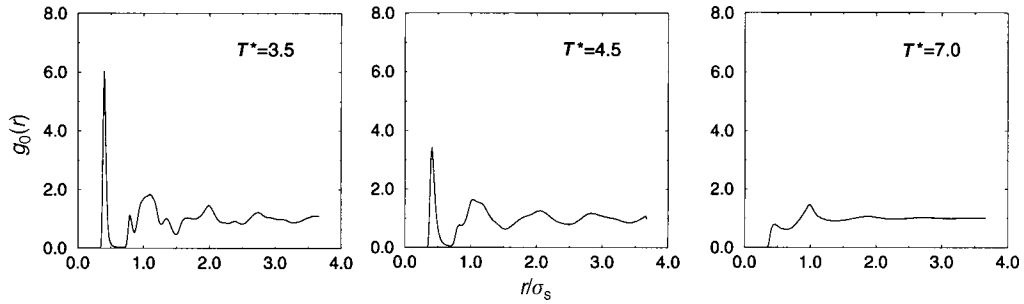

Fig. 3 Radial correlation function $g_0(r)$ for a system of $N = 1000$ dipolar GB discs with transverse dipole $\mu^* = 0.8$ at $\rho^* = 2.5$ and temperatures $T^* = 3.5$ (left), 4.5 (middle) and 7.0 (right).

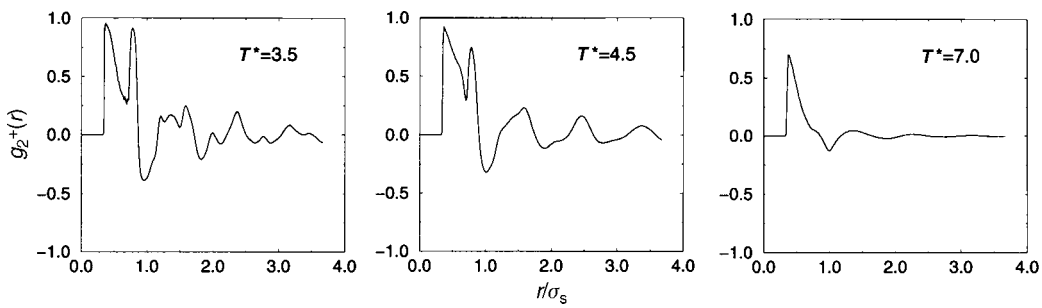

Fig. 4 Second rank anisotropy of the pair correlation $g_2{}^+(r)$. See Fig. 3 for details.

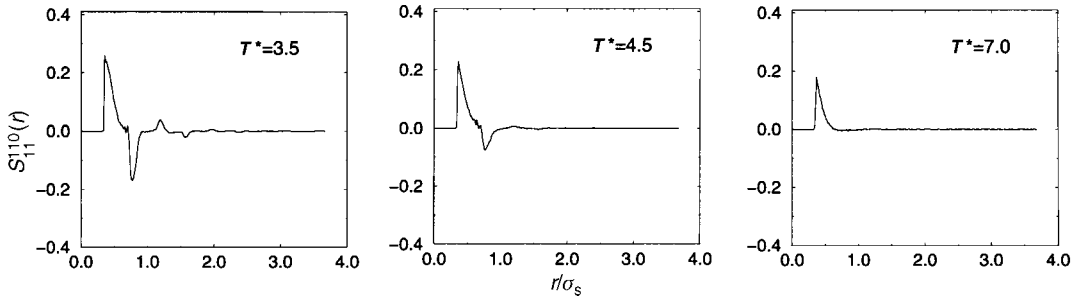

Fig. 5 Orientational correlation function $S_{11}^{110}(r)$. See Fig. 3 for details.

with respect to the pair distribution function $P(r, \omega_i, \omega_j, \omega_r)$ over molecular orientations ω_i, ω_j and intermolecular vector orientation ω_r.[13] We consider in particular the $S_{11}^{110}(r)$, $S_{00}^{220}(r)$, $S_{22}^{220}(r)$, that we now introduce in turn. We start with the first rank invariant (the real part is shown)

$$S_{11}^{110}(r) = -\frac{1}{2\sqrt{3}} \langle \delta(r - r_{ij})[(\hat{\boldsymbol{x}}_i \cdot \hat{\boldsymbol{x}}_j) - (\hat{\boldsymbol{y}}_i \cdot \hat{\boldsymbol{y}}_j)] \rangle_{ij}, \quad (4)$$

that depends on the biaxial orientational correlations between dipoles $\boldsymbol{\mu}_i \| \hat{\boldsymbol{x}}_i$ as a function of the molecular separation r and that we report in Fig. 5. At temperature $T^* = 3.5$ this function presents a well defined positive peak followed by a second one of opposite sign. This corresponds to an intra-column pairing of neighbouring dipoles with anti-parallel dipole moments. This arrangement, if propagated, could lead to phase biaxiality. However, as already mentioned, the long range phase biaxiality measured by $\langle R_{22}^2 \rangle$ turned out to be zero. A similar short range structure can be found at the intermediate temperature $T^* = 4.5$ but the dipole–dipole correlation vanishes after the second intra-column neigbours and the overall phase biaxiality is again practically absent (*cf.* Table 1). In the nematic phase ($T^* = 7.0$) the anti-ferroelectric arrangement is even more short ranged and the phase is on the whole uniaxial.

As for second rank invariants we concentrate on

$$S_{00}^{220}(r) = \frac{1}{2\sqrt{5}} \langle \delta(r - r_{ij})[3(\hat{\boldsymbol{z}}_i \cdot \hat{\boldsymbol{z}}_j)^2 - 1] \rangle_{ij}, \quad (5)$$

and (the real part is shown)

$$\begin{aligned} S_{22}^{220}(r) = \frac{1}{4\sqrt{5}} \langle \delta(r - r_{ij}) \\ \times [(\hat{\boldsymbol{x}}_i \cdot \hat{\boldsymbol{x}}_j)^2 - (\hat{\boldsymbol{x}}_i \cdot \hat{\boldsymbol{y}}_j) - (\hat{\boldsymbol{y}}_i \cdot \hat{\boldsymbol{x}}_j)^2 \\ + (\hat{\boldsymbol{y}}_i \cdot \hat{\boldsymbol{y}}_j)^2 - 2(\hat{\boldsymbol{x}}_i \cdot \hat{\boldsymbol{y}}_j)(\hat{\boldsymbol{y}}_i \cdot \hat{\boldsymbol{x}}_j) \\ - 2(\hat{\boldsymbol{x}}_i \cdot \hat{\boldsymbol{x}}_j)(\hat{\boldsymbol{y}}_i \cdot \hat{\boldsymbol{y}}_j)] \rangle_{ij}. \end{aligned} \quad (6)$$

We have reported the explicit expression for the invariants using a cartesian representation in terms of the molecular versor axes $\hat{\boldsymbol{x}}_i$, $\hat{\boldsymbol{y}}_i$ and $\hat{\boldsymbol{z}}_i$. However, to establish a relation between the long molecular distance values of the invariants and the other parameters we recall that in general these invariant functions are defined as linear combinations of products of Wigner matrices.[26,28,29] The average behaviour for large separations $r \ll \sigma_s$ is determined by the fact that the pair distribution becomes a product of singlet orientational distributions, which implies that the long distance values can be written in terms of products of orientational order parameters

$$S_{n_1 n_2}^{220}(r) \to \sum_m C(220; m, -m) \langle R_{m,n_1}^2 \rangle \langle R_{m,n_2}^2 \rangle, \quad (r \gg \sigma_s) \quad (7)$$

where $C(220; m, -m)$ are Clebsch–Gordan coefficients.[26] In particular we have

$$S_{00}^{220}(r) \to \frac{1}{\sqrt{5}} [\langle R_{00}^2 \rangle^2 + 2\langle R_{20}^2 \rangle^2], \quad (r \gg \sigma_s) \quad (8)$$

$$S_{22}^{220}(r) \to \frac{1}{\sqrt{5}} [\langle R_{02}^2 \rangle^2 + 2\langle R_{22}^2 \rangle^2]. \quad (r \gg \sigma_s) \quad (9)$$

In Fig. 6 we report the rotational invariants $S_{00}^{220}(r)$ and $S_{22}^{220}(r)$ for the temperatures $T^* = 3.5$, 4.5 and 7.0. The lowest temperature would seem to indicate a small biaxial order, but the values are essentially within the threshold error level of the simulation, confirming once more the uniaxial character of the phase.

4 External field effects

As we have seen in previous sections the systems studied show local but not overall biaxial structuring in the absence of a symmetry breaking field. On the other hand what is potentially interesting also for applications is the possibility of switching from uniaxial to biaxial following an external stimulus. Thus, in a second set of simulations we have studied the effect on the molecular and dipolar organization caused by the application of an external transversal field. The field coupling contribution for each molecule can be considered as the

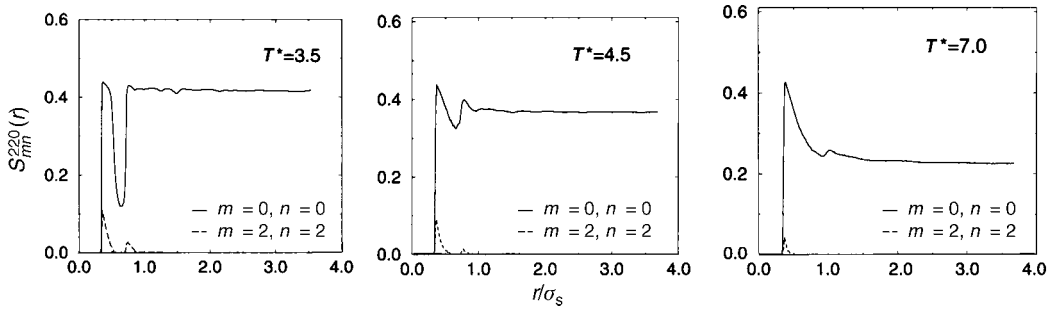

Fig. 6 Orientational correlation functions $S_{00}^{220}(r)$ (solid line) and $S_{22}^{220}(r)$ (dashed line). See Fig. 3 for details.

first anisotropic and non-polar term of a general expansion of the interaction energy in powers of field strength $E^* = (\sigma_s^3/\varepsilon_s)^{1/2}E$ (ref. 30)

$$U_i^{f*} = -\lambda D_{00}^2(\hat{\boldsymbol{x}}_i \cdot \hat{\boldsymbol{X}}), \quad (10)$$

where the field is applied transversally, along the $\hat{\boldsymbol{X}}$ direction of the director frame. We envisage a situation where an electric field $\boldsymbol{E}$ couples with the molecular dipole through a dielectric mechanism and where the unperturbed state is not polar overall, with $\lambda = \mu^{*2}E^{*2}/3$ is the field–dipole coupling strength.[30,31]

We have considered first a system of $N = 1000$ particles in the isobaric–isothermal (NPT) ensemble enclosed in a box with periodic boundary conditions and dimensionless pressure $P^* = 5$. We have chosen to concentrate on the state point temperature $T^* = 3.5$, and we have performed a set of simulations for various values of the applied field and for two different values of the dipole moment $\mu^* = 0.8$ and $\mu^* = 0.4$. For $\mu \approx 1.6$ D (*i.e.* $\mu^* = 0.8$), $\lambda = 1$ corresponds to an electric field $E \approx 160$ V μm^{-1}. Lower fields could be achieved with stronger molecular dipoles.

Then we have repeated the simulation with the stronger dipole moment for a system with a large number of particles ($N = 8000$).

In Table 2 we report the equilibrium results for the energy and the two main order parameters. It is immediately apparent that when the transversal field is applied, the phase becomes biaxial (see Fig. 7 and also the configurations in Fig. 8) and that the induced biaxiality changes quite considerably when the dipole moment is increased from $\mu^* = 0.4$ to $\mu^* = 0.8$, as shown in Fig. 7.

We notice that this symmetry change does not involve much of a change in the structural organization of the phase and the principal order parameter $\langle R_{00}^2 \rangle$ in Table 2 is practically unaffected by the external field. Indeed, in Fig. 9 we see that the radial distribution is essentially the same also for the strongest applied field, where the contribution of the field term

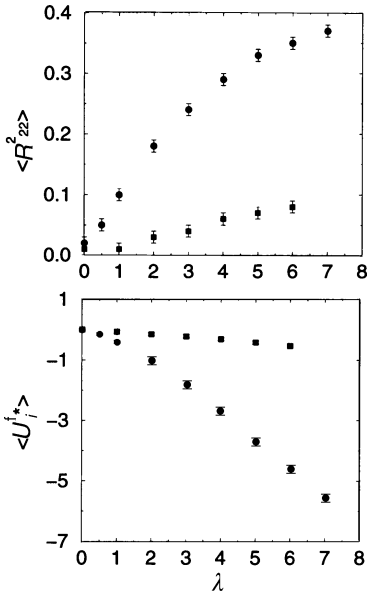

Fig. 7 Biaxial order parameter $\langle R_{22}^2 \rangle$ (top) and field interaction energy per molecule $\langle U_i^{f*} \rangle$ (bottom) as a function of the field–dipole coupling strength λ for a system of $N = 1000$ dipolar GB discs as a function of the field–dipole coupling strength $\lambda = \mu^{*2}E^{*2}/3$ at pressure $P^* = 5$, temperature $T^* = 3.5$ and for transverse dipole moments $\mu^* = 0.8$ (circles) and 0.4 (squares).

to the total energy (Table 2) is far from negligible. Also the plot of $S_{11}^{110}(r)$ in Fig. 10 shows similar profiles for each value of λ, while $S_{22}^{220}(r)$ (plotted in Fig. 11) has not zero limiting values for large intermolecular separations, in agreement with eqn. (9). It is thus reasonable to treat the effect of the transverse field in terms of linear response theory[17,32–34] and we now proceed to calculating this response property establishing first its formulation in molecular terms.

Table 2 Results of MC-NPT simulations in the presence of an external transversal field at pressure $P^* = 5$ and temperature $T^* = 3.5$ for a columnar phase with $N = 1000$ GB discotic molecules with transversal dipole: $\mu^* = 0.8$ (2a), and $\mu^* = 0.4$ (2b), and of $N = 8000$ with $\mu^* = 0.8$ (2c). The constant $\lambda = \mu^{*2}E^{*2}/3$ defines the field–dipole coupling strength. We report the average Gay–Berne $\langle U_{ij}^{GB*} \rangle$, dipolar $\langle U_{ij}^{d*} \rangle$ and field $\langle U_i^{f*} \rangle$ energies per particle and the orientational order parameters $\langle R_{00}^2 \rangle$ and $\langle R_{22}^2 \rangle$. Additional biaxial order parameters $\langle R_{02}^2 \rangle$ and $\langle R_{20}^2 \rangle$ are zero, within the simulation error bars, at all applied fields

λ	$\langle U_{ij}^{GB*} \rangle$	$\langle U_{ij}^{d*} \rangle$	$\langle U_i^{f*} \rangle$	$\langle R_{00}^2 \rangle$	$\langle R_{22}^2 \rangle$
2a					
0.0	−31.9 ± 0.2	−6.0 ± 0.1	—	0.96 ± 0.01	0.02 ± 0.01
0.5	−32.0 ± 0.2	−6.0 ± 0.1	−0.15 ± 0.05	0.96 ± 0.01	0.05 ± 0.01
1.0	−32.1 ± 0.2	−6.1 ± 0.1	−0.40 ± 0.05	0.97 ± 0.01	0.10 ± 0.01
2.0	−32.2 ± 0.2	−6.2 ± 0.1	−1.0 ± 0.1	0.97 ± 0.01	0.18 ± 0.01
3.0	−32.5 ± 0.2	−6.5 ± 0.1	−1.8 ± 0.1	0.97 ± 0.01	0.24 ± 0.01
4.0	−32.5 ± 0.2	−6.7 ± 0.1	−2.7 ± 0.1	0.97 ± 0.01	0.29 ± 0.01
5.0	−32.6 ± 0.2	−6.8 ± 0.1	−3.7 ± 0.1	0.97 ± 0.01	0.33 ± 0.01
6.0	−32.8 ± 0.2	−7.0 ± 0.1	−4.6 ± 0.1	0.97 ± 0.01	0.35 ± 0.01
7.0	−33.2 ± 0.2	−7.3 ± 0.1	−5.6 ± 0.1	0.97 ± 0.01	0.37 ± 0.01
2b					
0.0	−26.4 ± 0.2	−0.5 ± 0.1	—	0.93 ± 0.01	0.01 ± 0.01
1.0	−26.8 ± 0.2	−0.5 ± 0.1	−0.07 ± 0.05	0.93 ± 0.01	0.01 ± 0.01
2.0	−26.4 ± 0.2	−0.5 ± 0.1	−0.15 ± 0.05	0.93 ± 0.01	0.03 ± 0.01
3.0	−26.7 ± 0.2	−0.5 ± 0.1	−0.22 ± 0.05	0.93 ± 0.01	0.04 ± 0.01
4.0	−26.6 ± 0.2	−0.5 ± 0.1	−0.31 ± 0.05	0.93 ± 0.01	0.06 ± 0.01
5.0	−26.8 ± 0.2	−0.5 ± 0.1	−0.42 ± 0.05	0.93 ± 0.01	0.07 ± 0.01
6.0	−26.8 ± 0.2	−0.5 ± 0.1	−0.53 ± 0.05	0.93 ± 0.01	0.08 ± 0.01
2c					
0.0	−32.6 ± 0.2	−6.1 ± 0.1	—	0.97 ± 0.01	0.01 ± 0.01
1.0	−32.7 ± 0.2	−6.1 ± 0.1	−0.40 ± 0.05	0.97 ± 0.01	0.10 ± 0.01
2.0	−32.8 ± 0.2	−6.3 ± 0.1	−1.0 ± 0.1	0.97 ± 0.01	0.18 ± 0.01
3.0	−32.9 ± 0.2	−6.5 ± 0.1	−1.8 ± 0.1	0.97 ± 0.01	0.24 ± 0.01
4.0	−33.1 ± .02	−6.8 ± 0.1	−2.7 ± 0.1	0.97 ± 0.01	0.29 ± 0.01
5.0	−33.2 ± 0.2	−6.9 ± 0.1	−3.7 ± 0.1	0.97 ± 0.01	0.33 ± 0.01

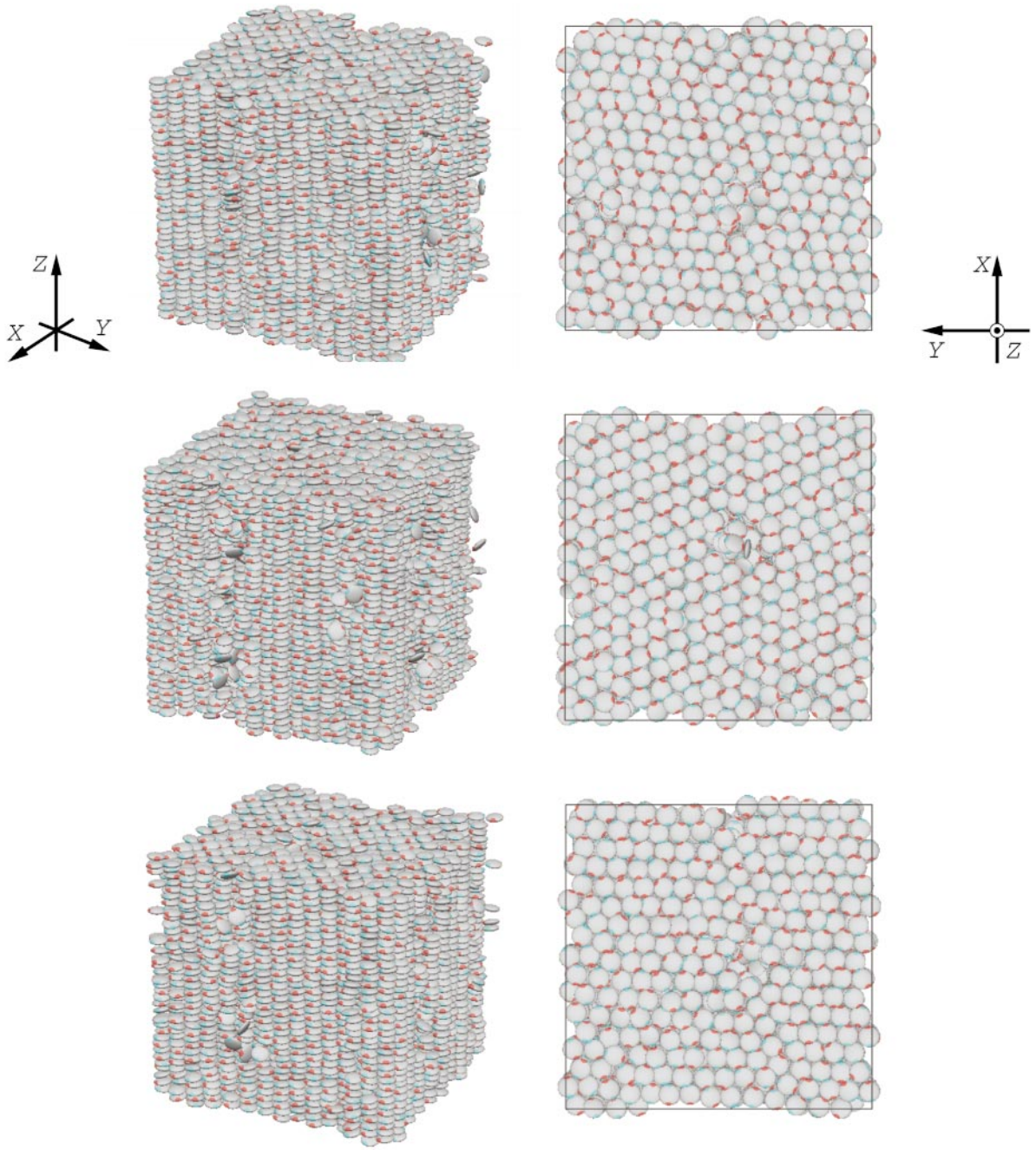

Fig. 8 Snapshots of MC-NPT configurations (side and top views) for columnar systems (aligned along $\hat{\boldsymbol{Z}}$) of $N = 8000$ dipolar GB discs with transverse dipole $\mu^* = 0.8$ at pressure $P^* = 5$, temperature $T^* = 3.5$ and external transversal field along $\hat{\boldsymbol{X}}$, for three values of the field–dipole coupling strength $\lambda = 0$ (top), 3 (middle), and 5 (bottom). The red and cyan "patches" label head and tail of molecular dipoles.

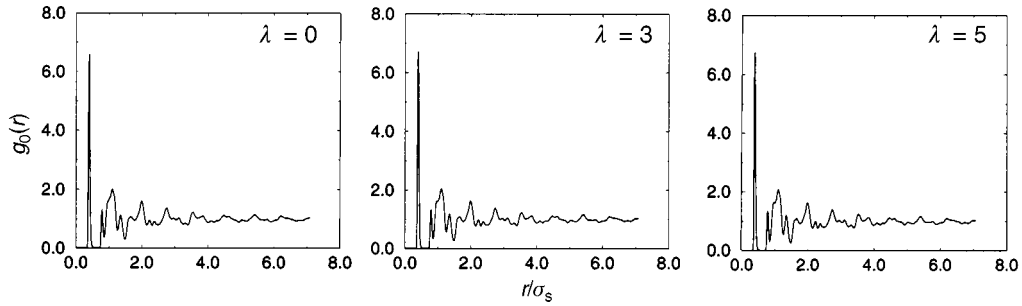

Fig. 9 Radial correlation function $g_0(r)$ for a system of $N = 8000$ dipolar GB discs with transverse dipole $\mu^* = 0.8$ at pressure $P^* = 5$, temperature $T^* = 3.5$ and three values of the field–dipole coupling strength $\lambda = 0$ (left), 3 (middle), and 5 (right).

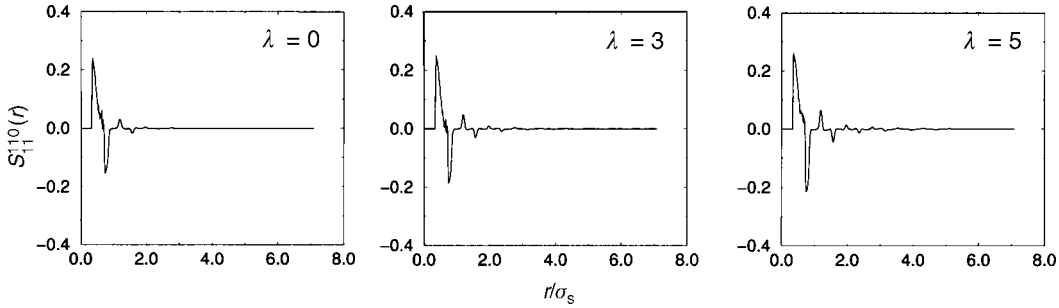

Fig. 10 Orientational correlation function $S_{11}^{110}(r)$. See Fig. 9 for details.

4.1 Linear field susceptibility

Here we derive an expression for the field susceptivity referring in particular to a columnar mesophase formed by discotic particles with transversal dipole moment and an external field orthogonal to the principal phase director $\hat{\boldsymbol{Z}}$. The unperturbed system has total energy given by the Hamiltonian

$$\mathscr{H} = \sum_{i=1}^{N-1} \sum_{j=i+1}^{N} U_{ij}, \tag{11}$$

where $U_{ij} = U_{ij}^{\mathrm{GB}} + U_{ij}^{\mathrm{d}}$. The mesophase symmetry of the unperturbed state is $D_{\infty\mathbf{h}}$ and it reduces to $D_{2\mathbf{h}}$ when the field (*cf.* eqn. (12)) is turned on. Using a laboratory/director frame L whose $\hat{\boldsymbol{Z}}$ axis is parallel to the column alignment axis, the Hamiltonian describing the interaction with the external transversal field aligned with respect to $\hat{\boldsymbol{X}}$ (the field frame F) is

$$\mathscr{H}_{\mathrm{f}} = -\frac{\mu^2 E^2}{3\varepsilon_{\mathrm{s}}} \sum_{i=1}^{N} D_{00}^2(\mathrm{x}_i \leftarrow \mathrm{F}) = -\frac{\mu^2 E^2}{3\varepsilon_{\mathrm{s}}}\, \phi(\{\omega\}), \tag{12}$$

where $\mathrm{x}_i \leftarrow \mathrm{F}$ stands for the rotation from the field frame to a molecular frame x_i with principal axis $\hat{\boldsymbol{x}}_i$. The symbol $\{\omega\}$ represents the set of all $3N$ Euler[26] angles defining the molecular orientations ω_i (*i.e.* the molecular fame M_i).

The average coupling term describing the overall interaction is

$$\langle\phi\rangle = \frac{1}{Z}\int \{\mathrm{d}\boldsymbol{r}\}\{\mathrm{d}\omega\}\phi(\{\omega\})\exp[-(\mathscr{H} + \mathscr{H}_{\mathrm{f}})/k_{\mathrm{B}}T], \tag{13}$$

where $\{\mathrm{d}\boldsymbol{r}\}$ and $\{\mathrm{d}\omega\}$ represent the integration over all $3N$ positional $\{\boldsymbol{r}\}$ and $3N$ orientational $\{\omega\}$ variables, while $Z = \int \{\mathrm{d}\boldsymbol{r}\}\{\mathrm{d}\omega\}\exp[-(\mathscr{H} + \mathscr{H}_{\mathrm{f}})/k_{\mathrm{B}}T]$ is the configurational integral.

Using linear response theory,[17,32–34] the susceptibility $\chi_\perp$ to the external transversal field is estimated as

$$\begin{aligned}\chi_\perp &= \frac{1}{N}\left[\frac{\partial\langle\phi\rangle}{\partial E^2}\right]_{E=0} = \left[\frac{\partial\langle D_{00}^2(\mathrm{x}_i \leftarrow \mathrm{F})\rangle}{\partial E^2}\right]_{E=0} \\ &= \frac{\mu^2}{3N\varepsilon_{\mathrm{s}}k_{\mathrm{B}}T}\left[\langle\phi^2\rangle - \langle\phi\rangle^2\right]_{E=0} \\ &= \frac{\mu^2}{3\varepsilon_{\mathrm{s}}k_{\mathrm{B}}T}\left[(N-1)c_{ij} + c_{ii}\right],\end{aligned} \tag{14}$$

where

$$c_{ij} \equiv \left[\langle D_{00}^2(\mathrm{x}_i \leftarrow \mathrm{F})D_{00}^2(\mathrm{x}_j \leftarrow \mathrm{F})\rangle - \langle D_{00}^2(\mathrm{x}_i \leftarrow \mathrm{F})\rangle^2\right] \tag{15}$$

and

$$c_{ii} \equiv \langle[D_{00}^2(\mathrm{x}_i \leftarrow \mathrm{F})]^2\rangle - \langle D_{00}^2(\mathrm{x}_i \leftarrow \mathrm{F})\rangle^2 \tag{16}$$

and we omit the $E = 0$ subscript since no confusion can arise. We have computed the coefficients c_{ij} and c_{ii} from the MC simulations results both from eqns. (15) and (16) and also by integration over the intermolecular distance r of appropriate orientational correlation functions (see Appendices 1 and 2 for details). Considering the effective phase and molecular biaxiality ($D_{2\mathbf{h}}$ symmetry), we expand the coefficients c_{ij} and c_{ii} in terms of a set of symmetrized biaxial invariants $R_{m_1m_2m_r;\, n_1n_2}^{L_1L_2L_r}$ resulting from the successive application of symmetry operators $\hat{\mathscr{P}}_{\mathrm{Mol}}^{D_{2\mathbf{h}}}$ and $\hat{\mathscr{P}}_{\mathrm{Lab}}^{D_{2\mathbf{h}}}$ to the product of three Wigner matrices $D_{m_1n_1}^{L_1*}(\omega_1)D_{m_2n_2}^{L_2*}(\omega_2)D_{m_r0}^{L_r*}(\omega_r)$ (see Appendix 2, eqn. (27)). Clearly this expansion is valid only for non-ferroelectric symmetry. Thus it is similar in spirit to the expansion of the singlet distribution in even Legendre polynomials, even if nematogen particles are polar. We obtain after some algebra and integration over the pair distribution function

$$\begin{aligned}c_{ij} = {} & \frac{1}{16}\langle R_{000;\,00}^{220}\rangle - \frac{\sqrt{3}}{4\sqrt{2}}\langle R_{000;\,20}^{220}\rangle + \frac{3}{8}\langle R_{000;\,22}^{220}\rangle \\ & - \frac{\sqrt{3}}{4\sqrt{2}}\langle R_{200;\,00}^{220}\rangle + \frac{3}{4}\langle R_{200;\,02}^{220}\rangle \\ & + \frac{3}{8}\langle R_{220;\,00}^{220}\rangle + \frac{3}{4}\langle R_{200;\,20}^{220}\rangle \\ & - \frac{3\sqrt{3}}{2\sqrt{2}}\langle R_{200;\,22}^{220}\rangle - \frac{3\sqrt{3}}{2\sqrt{2}}\langle R_{220;\,20}^{220}\rangle + \frac{9}{4}\langle R_{220;\,22}^{220}\rangle \\ & - \left[\frac{1}{4}\langle R_{00}^{2}\rangle - \sqrt{\frac{3}{8}}\langle R_{20}^{2}\rangle - \sqrt{\frac{3}{8}}\langle R_{02}^{2}\rangle + \frac{3}{2}\langle R_{22}^{2}\rangle\right]^2,\end{aligned} \tag{17}$$

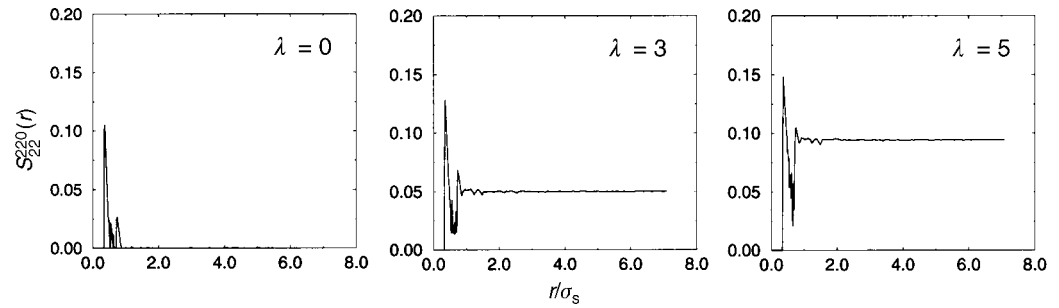

Fig. 11 Orientational correlation function $S_{22}^{220}(r)$. See Fig. 9 for details.

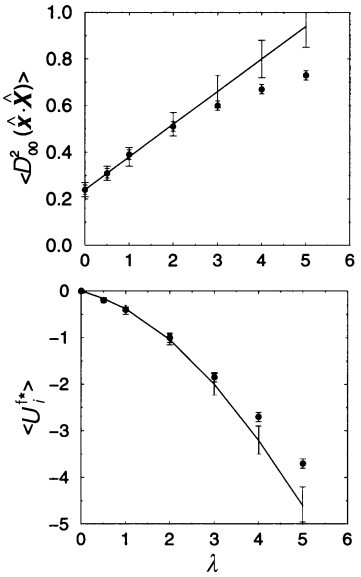

Fig. 12 Transversal order parameter $\langle D^2_{00}(\hat{\mathbf{x}}\cdot\hat{\mathbf{X}})\rangle$ (top) and average field energy per particle $\langle U_i^{f*}\rangle$ (bottom) computed directly from the MC-NPT simulations of $N = 1000$ GB discs with transverse dipole $\mu^* = 0.8$ at pressure $P^* = 5$, temperature $T^* = 3.5$ and different field–dipole coupling strengths λ (circles, *cf.* Table 2) and from the linear response susceptibility of an unperturbed ($\lambda = 0$) system (continuous curve, *cf.* eqns. (19) and (20)) with $\chi^*_\perp = (2.6 \pm 0.3) \times 10^{-2}$.

and

$$c_{ii} = \frac{1}{5} + \frac{1}{14}\left[\langle R^2_{00}\rangle - \sqrt{6}\langle R^2_{02}\rangle - \sqrt{6}\langle R^2_{20}\rangle + 6\langle R^2_{22}\rangle\right] + \frac{9}{1120}\left[9\langle R^4_{00}\rangle - 6\sqrt{10}\langle R^4_{02}\rangle + 3\sqrt{70}\langle R^4_{04}\rangle - 6\sqrt{10}\langle R^4_{20}\rangle + 40\langle R^4_{22}\rangle - 20\sqrt{7}\langle R^4_{2,4}\rangle + 3\sqrt{70}\langle R^4_{4,0}\rangle - 20\sqrt{7}\langle R^4_{4,2}\rangle + 70\langle R^4_{4,4}\rangle\right] - \left[\frac{1}{4}\langle R^2_{00}\rangle - \sqrt{\frac{3}{8}}\langle R^2_{20}\rangle - \sqrt{\frac{3}{8}}\langle R^2_{02}\rangle + \frac{3}{2}\langle R^2_{22}\rangle\right]^2, \quad (18)$$

where R^L_{mn} are the symmetrized Wigner matrices already defined in eqn. (3).

The dimensionless susceptibility $\chi^*_\perp = (\varepsilon_s/\sigma_s^3)\chi_\perp$ is a non-negative quantity ranging between 0 and $N\mu^{*2}c_{ii}/3T^*$, *i.e.* the limiting values for a system of particles whose orientational pair distribution is either completely uncorrelated or completely correlated. Considering GB discs with transverse dipole moment $\mu^* = 0.8$ at pressure $P^* = 5$ and temperature $T^* = 3.5$, we have found for the susceptibilities of two systems of $N = 1000$ and $N = 8000$ particles the same value $\chi^*_\perp = (2.6 \pm 0.3) \times 10^{-2}$, both by direct computation of eqns. (15) and (16) and by eqns. (17) and (18) after integration of the orientational correlation functions of Appendix 2.

Once the susceptibility is known, we can get for each field–dipole coupling strength λ, the transversal order parameter $\langle D^2_{00}(\hat{\mathbf{x}}\cdot\hat{\mathbf{X}})\rangle_\lambda$. Thus

$$\langle D^2_{00}(\hat{\mathbf{x}}\cdot\hat{\mathbf{X}})\rangle_\lambda - \langle D^2_{00}(\hat{\mathbf{x}}\cdot\hat{\mathbf{X}})\rangle_{\lambda=0} = \frac{3\lambda\chi^*_\perp}{\mu^{*2}}, \quad (19)$$

and then estimate the field coupling term $\langle U_i^{f*}\rangle_\lambda$ from the corresponding values in the absence of field

$$\langle U_i^{f*}\rangle_\lambda = -\lambda\langle D^2_{00}(\hat{\mathbf{x}}\cdot\hat{\mathbf{X}})\rangle_\lambda. \quad (20)$$

In Fig. 12 we report as functions of the parameter λ the estimated values from linear response theory of these two quantities compared with the ones obtained directly from simulations in the presence of a field. We can see that at least at low fields these results are fully consistent, thus confirming the applicability of the linear response equations.

It is worth noticing that the molecular expression we have established could be useful in analyzing experimental results for real columnar systems with a transverse dipole in a transversal field. Indeed, eqns. (14)–(18) provide a link between an observable susceptibility $\chi_\perp$ and single molecule and pair correlation properties. As an example of that, we show in Figs. (13) and (14) the biaxial invariants $R^{220}_{200;\,20}(r)$ and $R^{220}_{220;\,22}(r)$, that, at least in the present case, are the dominant biaxial terms in eqn. (17).

5 Conclusions

We have shown that a system of attractive–repulsive Gay–Berne discotic particles with an embedded transverse electric

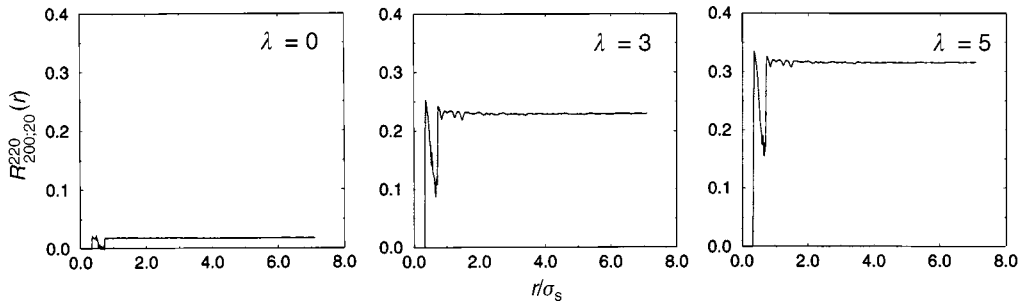

Fig. 13 Transversal orientational correlation function $R^{220}_{200;\,20}(r)$. See Fig. 9 for details.

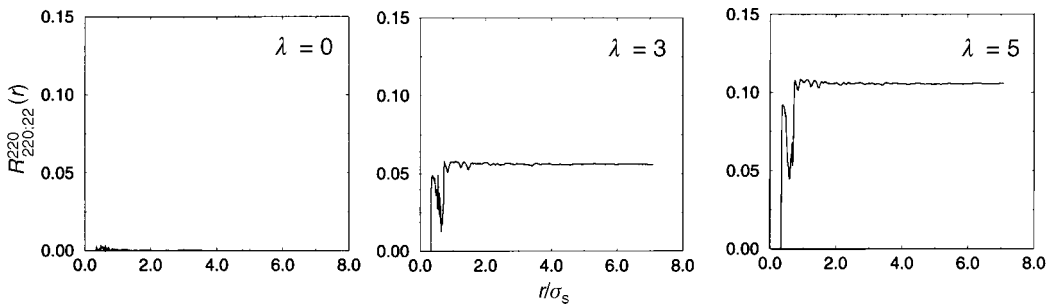

Fig. 14 Transversal orientational correlation function $R^{220}_{220;\,22}(r)$. See Fig. 9 for details.

dipole can form nematic and hexagonal columnar mesophases. In the absence of a field the system is uniaxial, although it presents a short range biaxial structure. At low temperatures, the columnar phase readily becomes biaxial when a transversal field is applied; the biaxiality increases with the field strength. The high susceptibility observed makes this type of polar discotics potentially interesting for uniaxial–biaxial switching applications.

6 Acknowledgements

We are grateful to NEDO (98MB1), University of Bologna, MURST PRIN Cristalli Liquidi, CNR PF MSTA-II, EU TMR (contract FMRX-CT97-0121) for support and CINECA for a generous grant of computer time on the Cray T3E 1200-256. We thank Prof. K. Praefcke and Dr. D. Blunk (TU Berlin) for useful discussions.

Appendix 1

We derive here some intermediate expression for the computation of the two particle averages c_{ij} and c_{ii} (eqns. (17) and (18)) required in the evaluation of the susceptibility according to the linear response theory.[17,32–34] The rotation matrices from the field to the molecular frame x_i can be rewritten as a sequence of three rotations[35] transforming first from the field F to the laboratory L, then from the laboratory L to the molecular M_i frames and finally from the molecular M_i to the molecular x_i frame

$$D^2_{00}(\mathrm{x}_i \leftarrow \mathrm{F}) = \sum_{p,\,q} D^2_{0p}(\mathrm{L} \leftarrow \mathrm{F}) D^2_{pq}(\mathrm{M}_i \leftarrow \mathrm{L}) D^2_{q0}(\mathrm{x}_i \leftarrow \mathrm{M}_i) = \sum_{p,\,q} a_p\, b_q\, D^2_{pq}(\omega_i), \tag{21}$$

where we have used $D^L_{mn}(\omega_i) \equiv D^L_{mn}(\mathrm{M}_i \leftarrow \mathrm{L})$, and introduced the shorthand

$$a_p = D^2_{0p}(\mathrm{L} \leftarrow \mathrm{F}) \equiv D^2_{0p}(0,\, -\pi/2,\, 0) = d^2_{0p}(-\pi/2), \tag{22}$$

$$b_q = D^2_{q0}(\mathrm{x}_i \leftarrow \mathrm{M}_i) \equiv D^2_{q0}(0,\, \pi/2,\, 0) = d^2_{q0}(\pi/2). \tag{23}$$

The distinct particle terms c_{ij} can be expressed as

$$\begin{aligned} c_{ij} &= \langle D^2_{00}(\mathrm{x}_i \leftarrow \mathrm{F}) D^2_{00}(\mathrm{x}_j \leftarrow \mathrm{F})\rangle - \langle D^2_{00}(\mathrm{x}_i \leftarrow \mathrm{F})\rangle^2 \\ &= \sum_{p_i,\,q_i,\,p_j,\,q_j} a_{p_i} b_{q_i} a_{p_j} b_{q_j} \langle D^2_{p_i q_i}(\omega_i) D^2_{p_j q_j}(\omega_j)\rangle \\ &\quad - \left[\sum_{p_i,\,q_i} a_{p_i} b_{q_i} \langle D^2_{p_i q_i}(\omega_i)\rangle\right]^2, \end{aligned} \tag{24}$$

while the self particle term c_{ii} is instead

$$\begin{aligned} c_{ii} &= \langle [D^2_{00}(\mathrm{x}_i \leftarrow \mathrm{F})]^2\rangle - \langle D^2_{00}(\mathrm{x}_i \leftarrow \mathrm{F})\rangle^2 \\ &= \sum_{p_i,\,q_i,\,p_j,\,q_j} a_{p_i} b_{q_i} a_{p_j} b_{q_j} \langle D^2_{p_i q_i}(\omega_i) D^2_{p_j q_j}(\omega_i)\rangle \\ &\quad - \left[\sum_{p_i,\,q_i} a_{p_i} b_{q_i} \langle D^2_{p_i q_i}(\omega_i)\rangle\right]^2 \\ &= \sum_{p_i,\,q_i,\,p_j,\,q_j} a_{p_i} b_{q_i} a_{p_j} b_{q_j} \sum_L C(22L;\, p_i\, p_j) \\ &\quad \times C(22L;\, q_i\, q_j) \langle D^L_{p_i + p_j,\, q_i + q_j}(\omega_i)\rangle \\ &\quad - \left[\sum_{p_i,\,q_i} a_{p_i} b_{q_i} \langle D^2_{p_i q_i}(\omega_i)\rangle\right]^2, \end{aligned} \tag{25}$$

where we have taken advantage of the Clebsch–Gordan coupling rule for Wigner matrices[26,36]

$$D^{L_i}_{p_i q_i}(\omega) D^{L_j}_{p_j q_j}(\omega) = \sum_{L=|L_i - L_j|}^{L_i + L_j} C(L_i\, L_j\, L;\, p_i\, p_j) C(L_i\, L_j\, L;\, q_i\, q_j) D^L_{p_i + p_j,\, q_i + q_j}(\omega). \tag{26}$$

Appendix 2

The susceptibility components c_{ii} and c_{ij} (eqns. (17) and (18)) can be evaluated by integration over the intermolecular distance r of certain orientational correlation functions, which in turn are the expansion coefficients of the pair distribution function $P(r,\, \omega_1,\, \omega_2,\, \omega_r)$ in a set of a suitably defined set of biaxial invariants. To build these invariants we generalize the procedure used for Stone invariants, derived in refs. 28 and 29, by spherical symmetrization of products of three Wigner matrices,[26,35] $D^{L_1 *}_{m_1 n_1}(\omega_1) D^{L_2 *}_{m_2 n_2}(\omega_2) D^{L_r *}_{m_r 0}(\omega_r)$. Here we derive in a similar way a set of biaxially symmetrized invariants, assuming that the phase and its constituent particles have effective $D_{2\mathrm{h}}$ symmetry. The application of projection operators gives the biaxial invariants as

$$\begin{aligned} R^{L_1 L_2 L_r}_{m_1 m_2 m_r;\, n_1 n_2} &= \hat{\mathscr{P}}^{D_{2\mathrm{h}}}_{\mathrm{Mol}} \hat{\mathscr{P}}^{D_{2\mathrm{h}}}_{\mathrm{Lab}} [D^{L_1 *}_{m_1 n_1}(\omega_1) D^{L_2 *}_{m_2 n_2}(\omega_2) D^{L_r *}_{m_r 0}(\omega_r)] \\ &= \tfrac{1}{4} \delta_{L_1 + L_2 + L_r,\, \mathrm{even}}\, \delta_{m_1 + m_2 + m_r,\, \mathrm{even}}\, \delta_{n_1,\, \mathrm{even}}\, \delta_{n_2,\, \mathrm{even}} \\ &\quad \times [\mathrm{Re}[D^{L_1 *}_{m_1,\, n_1}(\omega_1) D^{L_2 *}_{m_2,\, n_2}(\omega_2) D^{L_r *}_{m_r,\, 0}(\omega_r)] \\ &\quad + \mathrm{Re}[D^{L_1 *}_{m_1,\, n_1}(\omega_1) D^{L_2 *}_{m_2,\, -n_2}(\omega_2) D^{L_r *}_{m_r,\, 0}(\omega_r)] \\ &\quad + \mathrm{Re}[D^{L_1 *}_{m_1,\, -n_1}(\omega_1) D^{L_2 *}_{m_2,\, n_2}(\omega_2) D^{L_r *}_{m_r,\, 0}(\omega_r)] \\ &\quad + \mathrm{Re}[D^{L_1 *}_{m_1,\, -n_1}(\omega_1) D^{L_2 *}_{m_2,\, -n_2}(\omega_2) D^{L_r *}_{m_r,\, 0}(\omega_r)]]\,. \end{aligned} \tag{27}$$

These functions are orthogonal, namely

$$\langle R^{L_1 L_2 L_r}_{m_1 m_2 m_r;\, n_1 n_2} \,|\, R^{L_1' L_2' L_r'}_{m_1' m_2' m_r';\, n_1' n_2'}\rangle = \delta_{\lambda,\, \lambda'} \frac{32\pi^5 (1 + \delta_{m_1,\,0}\, \delta_{m_2,\,0}\, \delta_{m_r,\,0})(1 + \delta_{n_1,\,0})(1 + \delta_{n_2,\,0})}{(2L_1 + 1)(2L_2 + 1)(2L_r + 1)} \tag{28}$$

where $\lambda \equiv (L_1 L_2 L_3,\, |m_1 \| m_2 \| m_r|;\, |n_1 \| n_2|)$. The pair distribution function can then be expanded as

$$\begin{aligned} P(r,\, \omega_1,\, \omega_2,\, \omega_r) &= 4\pi\rho g_0(r) \\ &\times \sum_{\substack{L_1,\, L_2,\, L_r \\ m_1, m_2, m_r \\ n_1, n_2}} \frac{(2L_1 + 1)(2L_2 + 1)(2L_r + 1)}{32\pi^2 (1 + \delta_{m_1,\,0}\, \delta_{m_2,\,0}\, \delta_{m_r,\,0})(1 + \delta_{n_1,\,0})(1 + \delta_{n_2,\,0})} \\ &\times R^{L_1 L_2 L_r}_{m_1 m_2 m_r;\, n_1 n_2}(r) R^{L_1 L_2 L_r *}_{m_1 m_2 m_r;\, n_1 n_2}(\omega_1,\, \omega_2,\, \omega_r), \end{aligned} \tag{29}$$

where the real expansion coefficients are

$$\begin{aligned} R^{L_1 L_2 L_r}_{m_1 m_2 m_r;\, n_1 n_2}(r) &= \frac{1}{4\pi\rho g_0(r)} \\ &\quad \times \int \mathrm{d}\omega_1\, \mathrm{d}\omega_2\, \mathrm{d}\omega_r\, P(r,\, \omega_1,\, \omega_2,\, \omega_r) \\ &\quad \times R_{m_1 m_2 m_r;\, n_1 n_2}(\omega_1,\, \omega_2,\, \omega_r), \end{aligned} \tag{30}$$

whose radial average is

$$\langle R^{L_1 L_2 L_r}_{m_1 m_2 m_r;\, n_1 n_2}\rangle = \frac{4\pi}{V} \int r^2\, \mathrm{d}r g_0(r) R^{L_1 L_2 L_r}_{m_1 m_2 m_r;\, n_1 n_2}(r). \tag{31}$$

In the limit of intermolecular distances larger than molecular dimensions $r \gg \sigma_\mathrm{s}$, the average coefficients converge to the product of two molecular (*i.e.* $\langle R^L_{mn}\rangle_{\omega_i}$) and one radial (*i.e.* $\langle R^L_{m0}\rangle_{\omega_r}$) orientational order parameters

$$R^{L_1 L_2 L_r}_{m_1 m_2 m_r;\, n_1 n_2}(r) \to \langle R^{L_1}_{m_1 n_1}\rangle_{\omega_i} \langle R^{L_2}_{m_2 n_2}\rangle_{\omega_i} \langle R^{L_r}_{m_r 0}\rangle_{\omega_r}, \quad (r \gg \sigma_\mathrm{s}) \tag{32}$$

and thus the average invariants will decay to zero if at least one of the order parameters averages to zero. Considering the effective phase and molecular biaxiality we can symmetrize the coefficients c_{ii} and c_{ij} (eqns. (24) and (25)) to get

$$\hat{\mathscr{P}}^{D_{2h}}_{\mathrm{Mol}}\hat{\mathscr{P}}^{D_{2h}}_{\mathrm{Lab}}c_{ij} = \sum_{p_i,\,q_i,\,p_j,\,q_j} a_{p_i}b_{q_i}a_{p_j}b_{q_j}\langle R^{220}_{p_ip_j0;\,q_iq_j}\rangle - \left[\sum_{p_i,\,q_i} a_{p_i}b_{q_i}\langle R^2_{p_iq_i}\rangle\right]^2, \tag{33}$$

and

$$\hat{\mathscr{P}}^{D_{2h}}_{\mathrm{Mol}}\hat{\mathscr{P}}^{D_{2h}}_{\mathrm{Lab}}c_{ii} = \sum_{p_i,\,q_i,\,p_j,\,q_j} a_{p_i}b_{q_i}a_{p_j}b_{q_j}\sum_{L=0}^{4} C(22L;\,p_ip_j) \times C(22L;\,q_iq_j)\langle R^L_{p_i+p_j,\,q_i+q_j}\rangle - \left[\sum_{p_i,\,q_i} a_{p_i}b_{q_i}\langle R^2_{p_iq_i}\rangle\right]^2. \tag{34}$$

After substitution of the explicit values for the small Wigner matrices[26,35] and Clebsch–Gordan coefficients[36] we get eqns. (17) and (18) for c_{ij} and c_{ii}.

We now list the explicit expressions for some rank two biaxial invariants

$$R^{220}_{000;\,00} = \tfrac{1}{4}[1 - 3A^{(1)2}_{zZ} - 3A^{(2)2}_{zZ} + 9A^{(1)2}_{zZ}A^{(2)2}_{zZ}] \tag{35}$$

$$R^{220}_{200;\,20} = \tfrac{1}{8}[2A^{(1)2}_{xY} + A^{(1)2}_{xZ} - 2A^{(1)2}_{yY} - A^{(1)2}_{yZ} - 6A^{(1)2}_{xY}A^{(2)2}_{zZ} - 3A^{(1)2}_{xZ}A^{(2)2}_{zZ} + 6A^{(1)2}_{yY}A^{(2)2}_{zZ} + 3A^{(1)2}_{yZ}A^{(2)2}_{zZ}] \tag{36}$$

$$\begin{aligned} R^{220}_{220;\,22} = \tfrac{1}{16}[&-4A^{(1)}_{xX}A^{(1)}_{xY}A^{(2)}_{xX}A^{(2)}_{xY} + 4A^{(1)}_{xX}A^{(1)}_{xY}A^{(2)}_{yX}A^{(2)}_{yY} \\ &+ 4A^{(1)}_{yX}A^{(1)}_{yY}A^{(2)}_{xX}A^{(2)}_{xY} - 4A^{(1)}_{yX}A^{(1)}_{yY}A^{(2)}_{yX}A^{(2)}_{yY} \\ &+ 4A^{(1)2}_{xY}A^{(2)2}_{xY} - 4A^{(1)2}_{xY}A^{(2)2}_{yY} - 4A^{(1)2}_{yY}A^{(2)2}_{xY} \\ &+ 4A^{(1)2}_{yY}A^{(2)2}_{yY} + 2A^{(1)2}_{xY}A^{(2)2}_{xZ} - 2A^{(1)2}_{xY}A^{(2)2}_{yZ} \\ &+ 2A^{(1)2}_{xZ}A^{(2)2}_{xY} - 2A^{(1)2}_{xZ}A^{(2)2}_{yY} - 2A^{(1)2}_{yY}A^{(2)2}_{xZ} \\ &+ 2A^{(1)2}_{yY}A^{(2)2}_{yZ} - 2A^{(1)2}_{yZ}A^{(2)2}_{xY} + 2A^{(1)2}_{yZ}A^{(2)2}_{yY} \\ &+ A^{(1)2}_{xZ}A^{(2)2}_{xZ} - A^{(1)2}_{xZ}A^{(2)2}_{yZ} - A^{(1)2}_{yZ}A^{(2)2}_{xZ} \\ &+ A^{(1)2}_{yZ}A^{(2)2}_{yZ}] \end{aligned} \tag{37}$$

where to keep the notation compact we use $\boldsymbol{A}^{(1)}$ and $\boldsymbol{A}^{(2)}$ for the cartesian rotation matrices that take molecules 1 and 2 from the laboratory to the molecular frame, and that have as elements the scalar products

$$A^{(i)}_{mL} = \langle m^{(i)}\,|\,L\rangle \tag{38}$$

with $\langle m^{(i)}\,| = \hat{\boldsymbol{x}}_i$, $\hat{\boldsymbol{y}}_i$ or $\hat{\boldsymbol{z}}_i$ the axes of molecular frame M_i, and $\langle L\,| = \hat{\boldsymbol{X}}$, $\hat{\boldsymbol{Y}}$ or $\hat{\boldsymbol{Z}}$ those of laboratory L frame.

References

1 S. Chandrasekhar, *Adv. Liq. Cryst.*, 1982, **5**, 47.
2 (*a*) M. Ebert, D. A. Jungbauer, K. Kleppinger, J. H. Wendorff, B. Kohne and K. Praefcke, *Liq. Cryst.*, 1989, **4**, 53; (*b*) K. Praefcke and J. D. Holbrey, *J. Inclusion Phenom. Mol. Recognit. Syst.*, 1996, **24**, 19 and refs. therein.
3 (*a*) H. Ringsdorf, R. Wüstefeld, E. Zerta, M. Ebert and J. H. Wendorff, *Angew. Chem. Int. Ed. Engl.*, 1989, **28**, 914; (*b*) P. Henderson, D. Beyer, U. Jonas, O. Karthaus, H. Ringsdorf, P. A. Heiney, N. C. Maliszewskyj, S. S. Ghosh, O. Y. Mindyuk and J. Y. Josefowicz, *J. Am. Chem. Soc.*, 1997, **119**, 4740.
4 S. A. Hudson and P. M. Maitlis, *Chem. Rev.*, 1993, **93**, 861.
5 (*a*) H. X. Zheng, P. J. Carroll and T. M. Swager, *Liq. Cryst.*, 1993, **14**, 1421; (*b*) S. T. Trzaska, H. Zheng and T. M. Swager, *Chem. Mater.*, 1999, **11**, 130.
6 (*a*) P. J. Alonso, M. Marcos, J. I. Martinez, V. M. Orera, M. L. Sanjuan and J. L. Serrano, *Liq. Cryst.*, 1993, **13**, 585; (*b*) M. A. Pérez-Jubindo, M. R. de la Fuente and M. Marcos, *Adv. Mater.*, 1994, **6**, 941.
7 N. Boden, R. J. Bushby and A. N. Cammidge, *Liq. Cryst.*, 1995, **18**, 673.
8 D. Guillon, *Structure and Bonding*, 1999, **95**, 42.
9 J. G. Gay and B. J. Berne, *J. Chem. Phys.*, 1981, **74**, 3316.
10 A. P. J. Emerson, G. R. Luckhurst and S. G. Whatling, *Mol. Phys.*, 1994, **82**, 113.
11 M. A. Bates and G. R. Luckhurst, *J. Chem. Phys.*, 1996, **104**, 6696.
12 M. A. Bates and G. R. Luckhurst, *Liq. Cryst.*, 1998, **24**, 229.
13 R. Berardi, S. Orlandi and C. Zannoni, *J. Chem. Soc., Faraday Trans.*, 1997, **93**, 1493.
14 R. Berardi, A. P. J. Emerson and C. Zannoni, *J. Chem. Soc., Faraday Trans.*, 1993, **89**, 4069.
15 G. Ayton and G. N. Patey, *Phys. Rev. Lett.*, 1996, **76**, 239.
16 (*a*) J. J. Weis, D. Levesque and G. J. Zarragoicoechae, *Phys. Rev. Lett.*, 1992, **69**, 913; (*b*) G. J. Zarragoicoechae, D. Levesque and J.J. Weis, *Mol. Phys.*, 1993, **78**, 1475.
17 D. Frenkel and B. Smit, *Understanding Molecular Simulation*, Academic Press, San Diego, 1996.
18 C. Bacchiocchi and C. Zannoni, *Phys. Rev. E*, 1998, **58**, 3257.
19 S. W. De Leeuw, J. W. Perram and E. R. Smith, *Proc. R. Soc. London Ser. A*, 1980, **373**, 27.
20 R. Berardi, S. Orlandi and C. Zannoni, *Chem. Phys. Lett.*, 1996, **261**, 363.
21 (*a*) J. A. Barker and R. O. Watts, *Mol. Phys.*, 1983, **26**, 789; (*b*) M. Neumannn, *Mol. Phys.*, 1983, **50**, 841.
22 A. Gil-Villegas, S. C. McGrother and G. Jackson, *Mol. Phys.*, 1997, **92**, 723.
23 M. Houssa, A. Oualid and L. F. Rull, *Mol. Phys.*, 1998, **94**, 439.
24 R. Berardi, S. Orlandi and C. Zannoni, *Int. J. Mod. Phys.* (*C*), 1999, **10**, 477.
25 F. Biscarini, C. Chiccoli, P. Pasini, F. Semeria and C. Zannoni, *Phys. Rev. Lett.*, 1995, **75**, 1803.
26 M. E. Rose, *Elementary Theory of Angular Momentum*, Wiley, New York, 1957.
27 A. P. J. Emerson, R. Hashim and G. R. Luckhurst, *Mol. Phys.*, 1992, **76**, 241.
28 A. J. Stone, *Mol. Phys.*, 1978, **36**, 241.
29 L. Blum and A. J. Torruella, *J. Chem. Phys.*, 1972, **56**, 303.
30 E. Berggren, C. Zannoni, C. Chiccoli, P. Pasini and F. Semeria, *Phys. Rev. E*, 1994, **49**, 614.
31 S. Chandrasekhar, *Liquid Crystals*, Cambridge University Press, Cambridge, 2nd edn., 1982.
32 R. Kubo, *Rep. Progr. Phys.*, 1966, **29**, 255.
33 H. L. Friedman, *A Course in Statistical Mechanics*, Prentice Hall, Englewood Cliffs, NJ, 1985.
34 C. Zannoni, in *Advances in the Computer Simulations of Liquid Crystals*, ed. P. Pasini and C. Zannoni, Kluwer, Dordrecht, 2000, ch. 2.
35 C. Zannoni, in *The Molecular Physics of Liquid Crystals*, ed. G. R. Luckhurst and G. W. Gray, Academic Press, London, 1979, ch. 3.
36 P. Pasini and C. Zannoni, "Tables of Clebsch Gordan Coefficients for Integer Angular Momentum $J = 0$–6", INFN Bull., TC-83/19, 1984.